

The ‘Friction’ of Vacuum, and other Fluctuation–Induced Forces

Mehran Kardar

Department of Physics, Massachusetts Institute of Technology, Cambridge, MA 02139

Ramin Golestanian

Institute for Advanced Studies in Basic Sciences, Zanjan 45195-159, Iran

(August 14, 2018)

The *static* Casimir effect describes an attractive force between two conducting plates, due to *quantum fluctuations* of the electromagnetic (EM) field in the intervening space. *Thermal fluctuations* of correlated fluids (such as critical mixtures, super-fluids, liquid crystals, or electrolytes) are also modified by the boundaries, resulting in finite-size corrections at criticality, and additional forces that effect wetting and layering phenomena. Modified fluctuations of the EM field can also account for the ‘van der Waals’ interaction between conducting spheres, and have analogs in the fluctuation–induced interactions between inclusions on a membrane. We employ a path integral formalism to study these phenomena for boundaries of arbitrary shape. This allows us to examine the many unexpected phenomena of the *dynamic* Casimir effect due to moving boundaries. With the inclusion of quantum fluctuations, the EM vacuum behaves essentially as a complex fluid, and modifies the motion of objects through it. In particular, from the mechanical response function of the EM vacuum, we extract a plethora of interesting results, the most notable being: **(i)** The effective mass of a plate depends on its shape, and becomes anisotropic. **(ii)** There is dissipation and damping of the motion, again dependent upon shape and direction of motion, due to emission of photons. **(iii)** There is a continuous spectrum of resonant cavity modes that can be excited by the motion of the (neutral) boundaries.

I. OUTLINE

Fluctuation-induced forces are ubiquitous in nature, covering many topics from biophysics to cosmology [1–5]. There are two basic ingredients in these phenomena: **(i)** A fluctuating medium, such as the electromagnetic (EM) field; and **(ii)** External objects whose presence suppresses (or in some way modifies) the fluctuations, such as dipoles or conductors. The overall strength of the interaction is proportional to the driving energy of fluctuations ($k_B T$ and \hbar for thermal and quantum fluctuations, respectively); its range is related to that of the correlations of the fluctuations. The most interesting cases are when the interactions are long–ranged, corresponding to scale free fluctuations.

The goal of this article is to provide a glimpse of the unity and simplicity of fluctuation–induced forces. While we attempt to describe a wide range of phenomena, this selection is by no means exhaustive, and highly biased by subjective interests. In the spirit of a colloquium, we have tried to avoid technical details, preferring to present dimensional arguments whenever possible. The interested reader is referred to various sources for calculational details.

A prototype of fluctuation–induced interactions is the Casimir force between conducting plates, due to *quantum fluctuations* of the EM field. In Sec.II we discuss several cases where the source of interaction is the *thermal fluctuations* of a correlated fluid between the bounding plates. This interaction was originally proposed for a liquid mixture at its critical point, but is also present when

long-range correlations appear as a result of symmetry breaking, as in *superfluids* or *liquid crystals*. There is even an attractive component to the (mainly repulsive) force between two similarly charged plates, due to fluctuations of counterions in a neutralizing solution. Since the latter connection is seldom made explicit, we expand on its origin in Appendix II. While the reader may skip any one of these sections without losing general track of the article, we note that experiments on wetting of helium films may provide a beautiful test of these forces.

The van der Waals and London dispersion forces between atoms and molecules can also be attributed to the modified fluctuations of the EM field. As we point out in Sec.III, there are analogous forces between inclusions on a membrane. Their origin is the modified *surface* fluctuations, and they decay more slowly with separation than the standard van der Waals interaction. We use this example to emphasize that *non-additivity* is an important feature of fluctuation–induced forces: they cannot be obtained from a pairwise sum of two-body potentials.

Many new results are obtained in going beyond the simple geometries of flat plates and simple spheres, by looking at rough and deformed structures, as in Sec.IV. Our key to implementing the corresponding non-standard boundary conditions is a path integral approach, which is sketched in Appendix A. This approach can also be used in conjunction with a path integral quantization of the electromagnetic field. Since in this relativistic theory, deformations in space and time appear on the same footing, we can examine the *dynamic Casimir* effect which is introduced in Sec.V.

Some of the unexpected phenomena that emerge from quantum fluctuations of the EM field in the presence of moving deformed plates are discussed in Sec.VI. There are corrections to the mass of a plate that depend on its shape. There is also dissipation due to emission of photons (which accounts for the ‘friction’ in the title of this article). While these effects are typically very small, we believe that they are significant for what they imply about the nature of the quantized EM vacuum. Qualitatively, with the inclusion of quantum fluctuation, the vacuum behaves as a complex fluid which influences the bodies moving through it.

II. FLUCTUATION-INDUCED FORCES

A. Quantum fluctuations

The standard Casimir effect [1,3] is a macroscopic manifestation of quantum fluctuations of vacuum. In 1948, Casimir considered the electromagnetic field in the cavity formed by two conducting plates at a separation H . Because the electric field must vanish at the boundaries, the normal modes of the cavity are characterized by wave-vectors $\vec{k} = (k_x, k_y, \pi n/H)$, with integer n . Once quantized, these normal modes can be regarded as harmonic oscillators of frequencies $\omega(\vec{k}) = c|\vec{k}|$; each of which in its ground state has energy $\hbar\omega(\vec{k})/2$. While adding up all the ground state energies leads to an infinite contribution to the overall energy $\mathcal{E}(H)$, Casimir showed that a finite *attractive* force is obtained from

$$F(H) = -\frac{\partial\mathcal{E}}{\partial H} = -\hbar c \times \frac{A}{H^4} \times \frac{\pi^2}{240}, \quad (1)$$

where A is the area of the plates. Thus, by measuring the mechanical force between macroscopic bodies, it is in principle possible to gain information about the behavior of the quantum vacuum.

The predictions of Casimir were followed by experiments on quartz [6] and aluminum [7] plates at separations $H > 10^3\text{\AA}$. However, these experiments, and others reviewed in Ref. [8], provided results that were at best in qualitative agreement with Eq.(1). It is only quite recently that high precision measurements of the force (using a torsion pendulum) between a gold plate, and gold plated sphere, confirmed the accuracy of the theoretical prediction to within %5 [9].

B. Thermal fluctuations

While the Casimir interaction is due to the *quantum fluctuations* of the electromagnetic field, there are several examples in *classical statistical mechanics*, where forces are induced by the *thermal fluctuations* of a correlated fluid. One of the best known examples comes from the

finite size corrections to the free energy at a critical point [4]. Fisher and de Gennes [10] argued that in a binary liquid mixture, the concentrations near a wall are perturbed only over a distance of the order of the correlation length ξ . Any interaction mediated by the concentration fluctuations must also decay with this characteristic length. However, at the critical point, where ξ diverges, they suggested an attractive contribution to the free energy of a critical film, that varies with its thickness H , as

$$\delta\mathcal{F}(H) = -k_B T \times \frac{A}{H^2} \times \Delta. \quad (2)$$

This is to be expected on dimensional grounds, as the free energy comes from thermal fluctuations, hence proportional to $k_B T$, and must be extensive in A . (Similar analysis in d -dimensions leads to a dependence as $1/H^{d-1}$.) In two dimensions, exact values for the dimensionless amplitude Δ can be obtained by employing techniques of conformal field theories [11]. In higher dimensions, they can be estimated numerically [12], and by $\epsilon = 4 - d$ expansions [13].

In analogy to the Casimir energy, we can regard Eq.(2) as due to the modified free energy of concentration fluctuations by the boundaries. However, the force that results from this free energy decays as $1/H^3$. The difference in power of H from Eq.(1) is explained by noting that the fluctuation energy in the latter is quantum in origin, hence proportional to $\hbar c$, which has dimensions of *energy times length*.

C. Superfluid films

In fact, long-range forces are induced by thermal fluctuations of any *correlated medium*, by which we mean any system with fluctuations that have long-range correlations [14]. The critical system is a very particular example; much more common are cases where long-range correlations exist due to Goldstone modes of a broken continuous symmetry, as in superfluids or liquid crystals. A superfluid is characterized by a complex order parameter, whose phase ϕ may vary across the system. The energy cost of such variations is governed by the Hamiltonian

$$\mathcal{H}[\phi] = \frac{K}{2} \int d^3\mathbf{x} (\nabla\phi)^2, \quad (3)$$

where the ‘‘phonon stiffness’’ K is related to the superfluid density. There is no characteristic length scale for fluctuations of ϕ , which scale as a power of the observation length. Consequently, we expect power law finite size scaling, just as in the case of a critical point. In the Casimir geometry, the free energy resulting from thermal fluctuations of these modes has the form [15]

$$\delta\mathcal{F}(H) = -k_B T \times \frac{A}{H^2} \times \frac{\zeta(3)}{16\pi}. \quad (4)$$

Note that the result is universal, i.e. independent of the stiffness K . A similar expression is obtained for the free energy of the electromagnetic field confined between metallic plates at high temperatures $k_B T \gg \hbar c/H$. However, the result is larger by a factor of two [16], reflecting the two polarizations of the normal modes (photons).

Liquid Helium is a powerful wetting agent, which tends to spread over most surfaces. The thickness of the wetting layer is controlled by the strength of the attractive forces that bind the film to the substrate [17], mostly due to van der Waals interactions. In the presence of a chemical potential penalty of $\delta\mu$ per unit volume, the energy of a film of thickness H is

$$\frac{E(H)}{k_B T} = A \left[\frac{\delta\mu}{k_B T} H + \frac{C}{H^2} \right], \quad (5)$$

where C is a *positive* numerical constant. Minimizing this expression leads to a thickness [18]

$$H = \left(\frac{2Ck_B T}{\delta\mu} \right)^{1/3}. \quad (6)$$

When the helium film is in the normal phase, the film thickness is determined solely by the strength of the van der Waals (vdW) force. The numerical value of $C_{>} = C_{vdW} > 0$ depends on the substrate, and is nonuniversal. However, when the film becomes superfluid, there is an additional attractive fluctuation-induced (FI) force due to Eq.(4), and $C_{<} = C_{vdW} + C_{FI}$; where $C_{FI} = -\zeta(3)/16\pi \approx -0.02391$. In the vicinity of the superfluid transition, there is a different attractive contribution to the force due to finite size scaling (FSS) of the critical fluctuations, as in Eq.(2), and $C_{\lambda} = C_{vdW} + C_{FSS}$. The best estimate for the finite size scaling amplitude for the XY model in $d = 3$ is $C_{FSS} \approx -0.03$ [19,20]. The parameter C thus takes three different values in the normal fluid, at the λ -point, and in the superfluid phase. From Eq.(6) we then expect *two* jumps in the film thickness, as the temperature is lowered through the superfluid transition. Experiments to monitor the film thickness, thus providing a test of these forces, are currently underway at Penn. State University [21].

D. Liquid crystals

Liquid crystals exemplify anisotropic cases of correlated fluids due to broken symmetry, which again lead to fluctuation-induced forces [23,24,15]. They are also easily accessible, as experiments can be performed at room temperature and require no fine tuning to achieve criticality. A *nematic* liquid crystal is composed of long molecules that are aligned, with an order parameter which is the ‘director’ field $\mathbf{n}(\mathbf{r})$, characterizing the local preferred direction of the long axis of the molecules [22]. The energy cost of fluctuations of this field is given by [22]

$$\mathcal{H}_N = \frac{1}{2} \int d^3\mathbf{r} \left[\kappa_1 (\nabla \cdot \mathbf{n})^2 + \kappa_2 (\mathbf{n} \cdot \nabla \times \mathbf{n})^2 + \kappa_3 (\mathbf{n} \times \nabla \times \mathbf{n})^2 \right]. \quad (7)$$

Integrating over the nematic fluctuations leads to a free energy contribution

$$\delta\mathcal{E}_N = -k_B T \times \frac{A}{H^2} \times \frac{\zeta(3)}{16\pi} \left(\frac{\kappa_3}{\kappa_1} + \frac{\kappa_3}{\kappa_2} \right). \quad (8)$$

Note that the resulting force does depend on the relative strengths of the elastic coupling constants (reflecting the anisotropy of the system).

In a smectic liquid crystal, the molecules segregate into layers which are fluid like. The fluctuations of these layers from perfect stacking are described by a scalar deformation $u(\mathbf{x}, z)$, which is subject to a Hamiltonian

$$\mathcal{H}_S = \frac{1}{2} \int d^3\mathbf{r} \left[B \left(\frac{\partial u}{\partial z} \right)^2 + \kappa (\nabla^2 u)^2 \right]. \quad (9)$$

The resulting interaction energy

$$\delta\mathcal{E}_S = -k_B T \times \frac{A}{H\lambda} \times \frac{\zeta(2)}{16\pi}, \quad \text{with } \lambda \equiv \sqrt{\frac{\kappa}{B}}, \quad (10)$$

falls off as $1/H$, reflecting the extreme anisotropy which has introduced an additional length scale λ into the problem. For potential experimental tests of these forces in surface freezing of liquid crystal films, see Ref. [25].

E. Charged fluids

Interactions between a collection of *charged macroions* in an aqueous solution of neutralizing *counterions*, with or without added salt, are in general very complex. The macroions may be charged spherical colloidal particles, charged amphiphilic membranes, stiff polyelectrolytes (e.g. microtubules, actin filaments, and DNA), or flexible polyelectrolytes (e.g. polystyrene sulphonate), and the counterions could be mono- or polyvalent. It is known that, under certain conditions, the accumulation (condensation) of counterions around highly charged macroions can turn the repulsive Coulomb interaction between them into an attractive one. The attractive interaction is induced by the diminished charge-fluctuations close to the macroions, (due to the condensation of counterions) [26–28], and in this sense related to the effects discussed in the previous sections.

Since the connection between the entropic attraction of charged macroions and the general class of fluctuation-induced forces, is seldom made explicit, in Appendix II we present a path integral formulation that makes this analogy more transparent. The interaction between macroions can be broken into two parts: A Poisson-Boltzmann (PB) free energy, and a fluctuation-induced

correction. Specifically, consider two parallel negatively charged 2D plates with densities $-\sigma$, separated by a distance H in $d = 3$, in a solution of neutralizing counterions with valence z . The PB equation can be solved exactly in this geometry, and the corresponding PB free energy, in the limit of highly charged plates, is [29]

$$F_{PB} = \frac{\pi}{2} \times \frac{A}{z^2 \ell_B H} \left[1 + \frac{1}{4\pi^2 \ell_B^2 z^2 \sigma^2 H^2} + \dots \right], \quad (11)$$

in which $\ell_B \equiv e^2/\epsilon k_B T$ is the Bjerrum length. Note that in the limit $\ell_B z \sigma H \gg 1$, the interaction is independent of the charge densities of the plates; i.e. it is *universal*.

The fluctuation-induced correction involves calculation of a determinant (see Appendix II), which depends on the local charge compressibilities. The true compressibility profile (and the charge density profile) emerging from the solution of the PB equation, is generally very complicated. It is usual to simplify the problem by assuming that the surface charge density is so high that the counterions are confined to a layer of thickness $\lambda \ll H$, where $\lambda \sim 1/z\ell_B\sigma$ is the Gouy-Chapman length. Then we can use an approximate compressibility profile $m^2(z) = (2/\xi)[\delta(z + H/2) + \delta(z - H/2)]$, in which $\xi^{-1} = \pi^2 \ell_B^2 z^2 \sigma^2 \lambda$ defines a ‘‘crossover length’’. In the limit $H/\xi \gg 1$, we again obtain [30]

$$F_{FI} = -k_B T \times \frac{A}{H^2} \times \frac{\zeta(3)}{16\pi} [1 + O(\xi/H)], \quad (12)$$

for the fluctuation-induced part of the interaction [31].

III. DISPERSION FORCES

A. Van der Waals interactions

In addition to his work on the force between plates, Casimir also realized [32] that the van der Waals and London [33] forces can also be understood on the same footing: The presence of the atoms modifies the fluctuations of the electromagnetic field, resulting in an attractive interaction. (For a modern perspective, see the discussion by Kleppner in Ref. [34].)

For example, let us consider two conducting spheres of volumes $V_1 = 4\pi a_1^3/3$ and $V_2 = 4\pi a_2^3/3$, at a distance R . Usually, the van der Waals interaction is obtained from the instantaneous induced dipoles on the spheres. However, it can be equivalently obtained by examining the electromagnetic fluctuations of the remaining space. The fluctuation induced interaction is proportional to the product of the excluded volumes, and thus on dimensional grounds we expect a potential

$$\mathcal{V}(R) = -k_B T \times \frac{V_1 V_2}{R^6} \times \Delta_T, \quad (13)$$

due to thermal fluctuations. When the fluctuations are of quantum origin, Eq.(13) is modified to

$$\mathcal{V}(R) = -\hbar c \times \frac{V_1 V_2}{R^7} \times \Delta_Q, \quad (14)$$

with $\Delta_Q = 23/(4\pi)$ [32].

Let us compare the above result with the more standard approach to calculating the London force between two neutral *atoms*: While the average dipole for each atom is zero, an instantaneous dipole fluctuation in one can induce a parallel instantaneous dipole on the other, leading to an attraction. Since the direct dipole-dipole interaction decays as $1/R^3$, the induced effect scales as the square, i.e. $1/R^6$. In this regards, it is similar to the result in Eq.(13), except that the characteristic energy is set by a typical atomic excitation energy of $\hbar\omega_0$ rather than $k_B T$. The retardation effects are then obtained by taking into account the finite speed of light. We can imagine that for large enough distances, when the signal goes from atom-1 to atom-2 to induce the dipole, and return to atom-1 to induce an attraction, it finds the dipole at atom-1 somewhat misaligned; resulting in a weaker attraction. The characteristic time for electron movements can be estimated from the frequency of the orbit as $\tau = 2\pi/\omega_0$. The crossover occurs when the travel time for the signal is comparable to this characteristic time, namely $R/c \sim \tau$. Hence, taking into account the retardation effect, the interaction is

$$\mathcal{V}_r(R) = -\hbar\omega_0 \times \frac{V_1 V_2}{R^6} \times f\left(\frac{R\omega_0}{c}\right). \quad (15)$$

The crossover function $f(x)$ is a constant for $x \rightarrow 0$, and vanishes as $1/x$ for $x \rightarrow \infty$. In the latter limit, the dependence on ω_0 vanishes, and the Casimir-Polder result of Eq.(14) is recovered. A similar crossover function between the two forms of interaction for conducting spheres in Eqs.(13) and (14), occurs at a distance $\lambda_T \sim \hbar c/k_B T$.

B. Inclusions on membranes

Dispersion forces are not limited to particles in three dimensional space, but also occur for inclusions on films and membranes, the latter is of potential importance for understanding the interactions between proteins floating on a cell membrane. A membrane is a bilayer of *amphiphilic* molecules, each composed of a *hydrophilic* or polar head, and a *hydrophobic* tail of hydrocarbon chains. The polar heads prefer to be in contact with the water, and in the bilayer structure insulate the ‘‘oily’’ hydrocarbon interior from contact with water. A bilayer that is in equilibrium with amphiphiles in solution, can easily change its area by exchanging molecules with this reservoir. This implies that the surface tension is zero [40–42], and the energy cost of deforming the bilayer is entirely due to bending [39]. The ‘‘flicker’’ of the membrane is thus governed by the elastic Hamiltonian

$$\mathcal{H} = \frac{\kappa}{2} \int d^2\mathbf{x} (\nabla^2 h(\mathbf{x}))^2, \quad (16)$$

where $h(\mathbf{x})$ is a height function describing deformations of the surface. Typical values of the bending rigidity κ , of biological membranes is of the order of $10^2 \text{ }^\circ K$.

Cell membranes also include proteins that perform various biological functions (e.g. pumps). Each protein inclusion disturbs the lipid bilayer, resulting in interactions between nearby inclusions (c.f. Refs. [35–38] and references therein). These disturbances, and the resulting interactions, tend to be short-ranged, falling off exponentially with a characteristic length related to the distance over which the lipid membrane “heals” [38]. There are also longer ranged interactions between the proteins: In addition to the standard van der Waals interaction, there are interactions mediated by the disturbed fluctuations of the flickering membrane. As discussed in Ref. [37], such interactions exist as long as the rigidity of the inclusion differs from that of the ambient membrane, and fall off as $1/R^4$. In particular, if the inclusions are much stiffer

than the membrane, the fluctuation-induced potential is

$$\mathcal{V}(R) = -k_B T \times \frac{A^2}{R^4} \times \frac{6}{\pi^2}, \quad (17)$$

where A is the area of each inclusion [44]. The interaction is attractive and independent of κ and $\bar{\kappa}$; its energy scale set by $k_B T$. A generalization of this result that includes quantum fluctuations of membranes is given in Ref. [45].

The form of the interaction depends sensitively on the shapes of the inclusions, as demonstrated by the calculation of the fluctuation-induced interaction between rod-like objects [43]. The rods are assumed to be sufficiently rigid so that they do not deform coherently with the underlying membrane. They can thus only perform rigid translations and rotations while remaining attached to the surface. As a result, the fluctuations of the membrane are constrained, having to vanish at the boundaries of the rods. Consider the situation depicted in Fig. 1, with two rods of lengths L_1 and L_2 at a separation $R \gg L_i$. The fluctuation-induced interaction is given by

$$V^T(R, \theta_1, \theta_2) = -\frac{k_B T}{128} \times \frac{L_1^2 L_2^2}{R^4} \times \cos^2 [2(\theta_1 + \theta_2)] + O\left(\frac{1}{R^6}\right), \quad (18)$$

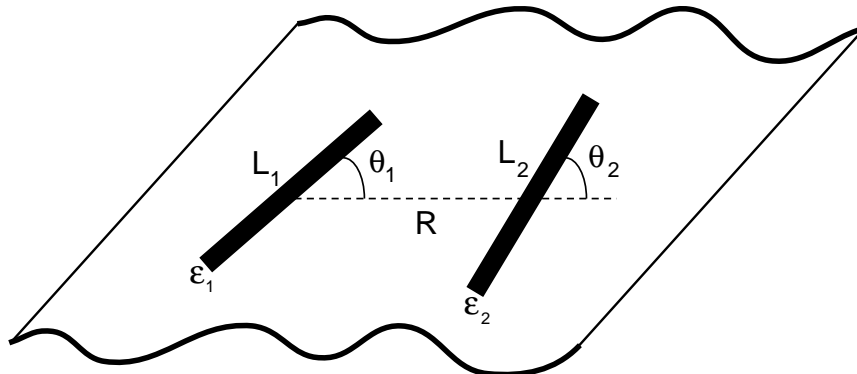


FIG. 1. Two rod-shaped inclusions embedded in a membrane. The rods are separated by a distance R . The i th rod has length L_i , width ϵ_i , and makes an angle θ_i with the line joining the centers of the two rods.

where θ_1 and θ_2 are the angles between the rods and the line adjoining their centers, as indicated in Fig. 1.

The orientational dependence is the *square* of a quadrupole–quadrupole interaction, with the unusual property of being minimized for both parallel and perpendicular orientations of the rods. The above fluctuation-induced interactions decay less rapidly at large distances than van der Waals forces and may play an important role in aligning asymmetric inclusions in biomembranes. Since orientational correlations are often easier to measure than forces, this result may also be useful as a probe of the fluctuation-induced interaction. Finally, this interaction could give rise to novel two-dimensional structures

for collections of rodlike molecules. In particular, the resemblance of the orientational part of the interaction to dipolar forces suggests that a suitable way to minimize the energy of a collection of rods is to form them into chains. (If the rods are not colinear, the interactions cannot be simultaneously minimized.)

An important property of fluctuation-induced interactions is that they are *non-additive*, and cannot be obtained by adding two-body potentials. For example, consider an interaction $U(|r_1 - r_2|) du_1 du_2$, between any two infinitesimal segments of two rods in Fig. 1. If both rods are of length L at a distance $R \gg L$, expanding $|r_1 - r_2|$, and integrating over the two rods, leads to the interaction

$$V(R, \theta_1, \theta_2) = L^2 U(R) + \frac{L^4}{6} \left(\frac{U'(R)}{R} + U''(R) \right) \quad (19)$$

$$- \frac{L^4}{12} \left(\frac{U'(R)}{R} - U''(R) \right) (\cos 2\theta_1 + \cos 2\theta_2).$$

The angular dependence is now completely different, and minimized when the two rods are parallel to their axis of separation. Presumably both interactions are present for rods of finite thickness; the additive interaction is proportional to $L^2(L\epsilon/R)^2$, where ϵ is the thickness. The previously calculated interactions are thus larger by a factor proportional to $(R/\epsilon)^2$ and should dominate at large separations.

The case of stiff linear inclusions at close separations ($L \gg R$) is considered in Ref. [46]. It is shown that a finite rigidity of the linear inclusions leads to a screening out of the Casimir-type fluctuation-induced attraction. The screening length is set by the ratio between the rigidity of the polymer and that of the membrane. This is the length scale below which the polymers are seen as straight parallel lines, hence resulting in a Casimir interaction. Moreover, the attractive interactions could lead to an instability in the shape of the stiff polymers signalling a major reduction in their rigidity (softening) induced by the membrane fluctuations [46].

IV. ROUGH SURFACES

Most computations of Casimir forces are for simple geometries, e.g. between two parallel plates, or perfect spheres. It is natural to consider how these forces are modified by the roughness that is present in most “random” surfaces. There are a number of calculations that go beyond the simple planar geometry. For example, in Ref. [47] a multiple scattering approach is used to compute the interactions for arbitrary geometry in a perturbation series in the curvature. A generalization of the approach due to Dzyaloshinskii, Lifshitz, and Pitaevskii [2] is developed in Ref. [48] to study the Casimir forces for surfaces with roughness. A phenomenological approach is introduced in Refs. [49] in which small deviations from plane parallel geometry are treated by using an additive summation of Casimir potentials. However (as demonstrated in the previous section), fluctuation induced forces are not additive, and additional steps are necessary to correct the result [49]. Another perturbative approach is introduced in Ref. [50], which could in principle be used to treat surfaces with roughness, although not explicitly carried out in this paper. Most of these approaches suffer from rather cumbersome treatments of the boundary conditions.

In Ref. [15], a path integral approach is introduced that makes possible relatively simple computations of the fluctuation induced force. (A sketch of this formulation is presented in Appendix A.) This approach has a number of advantages. First, different manifolds (with arbitrary

intrinsic and embedding dimensions) in various correlated fluids can be treated in a similar fashion. Second, the boundary conditions are quite easily implemented, and the corrections can be computed perturbatively in the deformations. While this method was originally developed for the study of thermal fluctuations, it can be adapted to quantum fluctuations, as discussed in the next section. In the remainder of this section we calculate the corrections to the thermal Casimir force due to substrate roughness.

Many solid surfaces produced by rapid growth or deposition processes are characterized by self-similar fluctuations [51]. The fluctuations of a self-affine surface grow as

$$\overline{[h(\mathbf{x}) - h(\mathbf{y})]^2} = A_S |\mathbf{x} - \mathbf{y}|^{2\zeta_S}, \quad (20)$$

where the overbar denotes quenched average, and ζ_S is a characteristic roughness exponent. The Casimir force between a flat and a such a rough surface (with a correlated fluid in between) is calculated in Ref. [15]. The resulting free energy per unit area is

$$\mathcal{F}(H) = -\frac{k_B T \zeta(3)}{H^2 16\pi} - \frac{k_B T A_S L^{2\zeta_S}}{H^4} \frac{3\zeta(3)}{16\pi} + \frac{k_B T A_S C_1}{H^{4-2\zeta_S} 4}, \quad (21)$$

where C_1 is a numerical coefficient [15], and L is the extent (upper cutoff) of the self-affine structure, satisfying $\Delta H \equiv A_S^{\frac{1}{2}} L^{\zeta_S} \ll H$. (This is the condition that the total width due to roughness, ΔH is less than the average separation H , so that the plates are not in contact.) As long as $L \gg H \gg \Delta H$, the interactions in Eq.(21) are arranged in order of increasing strength. The largest effect of randomness is to increase the Casimir attraction by an amount proportional to $(\Delta H/H)^2$. There is also another correction term, of the opposite sign, that decays as $1/H^{4-2\zeta_S}$, and in principle can be used to indirectly measure the roughness exponent ζ_S . In Eq.(20), if all lengths are measured in units of an atomic scale a_0 (e.g. the diameter of a surface atom), A_S becomes dimensionless. Using a reasonable set of parameters: $\zeta_S \approx 0.35$, $a_0 \approx 5\text{\AA}$, $A_S \approx 1$ and $L \approx 300\text{\AA}$, we estimate that for surfaces of 1mm size, and 100 \AA apart, the forces generated by the three terms in Eq.(21) are 1.9×10^{-4} , 4.9×10^{-5} , and $3.7 \times 10^{-6}\text{N}$ respectively, (using a reasonable lower cutoff of $\sim 20\text{\AA}$), which is measurable with the current force apparatus [9].

V. THE DYNAMIC CASIMIR EFFECT

A. Background

Although less well known than its static counterpart, the dynamical Casimir effect, describing the force and radiation from moving mirrors has also garnered much attention [52–58]. This is partly due to connections

to Hawking and Unruh effects (radiation from black holes and accelerating bodies, respectively), suggesting a deeper link between quantum mechanics, relativity, and cosmology [59,5].

The creation of photons by moving mirrors was first obtained by Moore [52] for a 1 dimensional cavity. Fulling and Davis [53] demonstrated that there is a corresponding force even for a single mirror, which depends on the third time derivative of its displacement. These computations take advantage of conformal symmetries of the 1+1 dimensional space time, and can not be easily generalized to higher dimensions. Furthermore, the calculated force has causality problems reminiscent of the radiation reaction forces in classical electron theory [54]. It has been shown that this problem is an artifact of the unphysical assumption of perfect reflectivity of the mirror, and can be resolved by considering realistic frequency dependent reflection and transmission from the mirrors [54].

Another approach to the problem starts with the fluctuations in the force on a single plate. The fluctuation–dissipation theorem is then used to obtain the mechanical response function [55], whose imaginary part is related to the dissipation. This method does not have any causality problems, and can also be extended to higher dimensions. (The force in 1+3 dimensional space-time depends on the fifth power of the motional frequency.) The emission of photons by a perfect cavity, and the observability of this energy, has been studied by different approaches [56–58]. The most promising candidate is the resonant production of photons when the mirrors vibrate at the optical resonance frequency of the cavity [59]. A review, and more extensive references are found in Ref. [60]. More recently, the radiation due to vacuum fluctuations of a collapsing bubble has been proposed [61–63] as a possible explanation for the intriguing phenomenon of sonoluminescence. (Subsequent experimental measurements of the duration of the signal [64] may favor more classical explanations.)

A number of authors have further discussed to notion of *frictional forces*: Using conformal methods in 1+1 dimensions, Ref. [65] finds a friction term

$$F_{\text{friction}}(H) = \alpha F_{\text{static}}(H) \left(\dot{H}/c \right)^2, \quad (22)$$

for slowly moving boundaries, where α is a numerical constant that only depends on dimensionality. The additional factor of $(v/c)^2$ makes detection of such a force yet more delicate. There are a few attempts to calculate forces (in higher dimensions) for walls that move *laterally*, i.e. parallel to each other [66–70]: It is found that *boundaries that are not ideal conductors* experience a friction as if the plates are moving in a viscous fluid. This friction has a complicated dependence on the frequency dependent resistivity of the plates, and vanishes in the cases of ideal (nondissipating) conductors or dielectrics. The “dissipation” mechanism for this “friction” is by inducing eddy currents in the nonideal conductors, and thus distinct from the Casimir effect. Possible experimental

evidence of such a contribution to friction has been recently reported in Ref. [71]. The experiment employs a quartz crystal microbalance technique to measure the friction associated with sliding of solid nitrogen along a lead surface, above and below the superconducting transition temperature of lead. An abrupt drop in friction is reported at the transition point as the substrate enters the superconducting state [71].

An interesting analog of the dynamic Casimir effect is suggested for the moving interface between two different vacuum states of superfluid ^3He [72]. In this system, the Andreev reflection of the massless “relativistic” fermions which live on the A-phase of the interface provides the corresponding mechanism for friction: The interface is analogous to a perfectly reflecting wall moving in the quantum vacuum.

B. Path integral formulation

The path integral methods originally developed for rough surfaces [73] can also be applied to the problem of perfectly reflecting mirrors that undergo arbitrary dynamic deformations. Consider the path integral quantization of a scalar field ϕ with the action

$$S = \frac{1}{2} \int d^4X \partial_\mu \phi(X) \partial_\mu \phi(X), \quad (23)$$

where summation over $\mu = 0, \dots, 3$ is implicit. Following a Wick rotation, imaginary time appears as another coordinate $X_4 = ict$, in the 4-dimensional space-time. In principle, we should use the electromagnetic vector potential $A_\mu(X)$, but requirements of gauge fixing complicate the calculations, while the final results only change by a numerical prefactor. (We have explicitly reproduced the known result for gauge fields between flat plates by this method [73].) We would like to quantize the field subject to the constraints of its vanishing on a set of n manifolds (objects) defined by $X = X_\alpha(y_\alpha)$, where y_α parametrize the α th manifold. We implement the constraints using delta functions, and write the partition function as

$$\mathcal{Z} = \int \mathcal{D}\phi(X) \prod_{\alpha=1}^n \prod_{y_\alpha} \delta(\phi(X_\alpha(y_\alpha))) \exp \left\{ -\frac{S[\phi]}{\hbar} \right\}. \quad (24)$$

The delta functions are next represented by integrals over Lagrange multiplier fields. Performing the Gaussian integrations over $\phi(X)$ then leads to an effective action for the Lagrange multipliers which is again Gaussian [15]. Evaluating \mathcal{Z} is thus reduced to calculating the logarithm of the determinant of a kernel. Since the Lagrange multipliers are defined on a set of manifolds with nontrivial geometry, this calculation is generally complicated. To be specific, we focus on two parallel 2d plates embedded in 3+1 space-time, and separated by an average distance H along the x_3 -direction. Deformations of the plates are parametrized by the height functions $h_1(\mathbf{x}, t)$ and

$h_2(\mathbf{x}, t)$, where $\mathbf{x} \equiv (x_1, x_2)$ denotes the two lateral space coordinates, while t is the time variable. As sketched in Appendix A, $\ln \mathcal{Z}$ can be calculated by a perturbative series in powers of the height functions [74]. The resulting

$$S_{\text{eff}} = \frac{\hbar c}{2} \int \frac{d\omega d^2 \mathbf{q}}{(2\pi)^3} [A_+(q, \omega) (|h_1(\mathbf{q}, \omega)|^2 + |h_2(\mathbf{q}, \omega)|^2) - A_-(q, \omega) (h_1(\mathbf{q}, \omega)h_2(-\mathbf{q}, -\omega) + h_1(-\mathbf{q}, -\omega)h_2(\mathbf{q}, \omega))] + O(\hbar^3). \quad (25)$$

C. The response function

The kernels $A_{\pm}(q, \omega)$, that are closely related to the mechanical response of the system (see below), are functions of the separation H , but depend on \mathbf{q} and ω only through the combination $Q^2 = q^2 - \omega^2/c^2$. The closed forms for these kernels involve cumbersome integrals, and are not very illuminating. Instead of exhibiting these formulas, we shall describe their behavior in various regions of the parameter space. In the limit $H \rightarrow \infty$, $A_{\pm}^{\infty}(q, \omega) = 0$, and

$$A_+^{\infty}(q, \omega) = \frac{1}{360\pi^2 c^5} \begin{cases} -(c^2 q^2 - \omega^2)^{5/2} & \text{for } \omega < cq, \\ i \operatorname{sgn}(\omega)(\omega^2 - c^2 q^2)^{5/2} & \text{for } \omega > cq, \end{cases} \quad (26)$$

where $\operatorname{sgn}(\omega)$ is the sign function. While the effective action is real for $Q^2 > 0$, it becomes purely imaginary for $Q^2 < 0$. The latter signifies dissipation of energy [55], presumably by generation of photons [58]. It agrees precisely with the results obtained previously [55] for the special case of flat mirrors ($\mathbf{q} = 0$). (Note that dissipation is already present for a single mirror.)

In the presence of a second plate (i.e. for finite H), the parameter space of the kernels subdivides into three different regions as depicted in Fig. 2. In region I ($Q^2 > 0$ for any H), the kernels are finite and real, and hence there is no dissipation. In region IIa where $-\pi^2/H^2 \leq Q^2 < 0$, the H -independent part of A_+ is imaginary, while the H -dependent parts of both kernels are real and finite. (This is also the case at the boundary $Q^2 = -\pi^2/H^2$.) The dissipation in this regime is simply the sum of what would have been observed if the individual plates were decoupled, and unrelated to the separation H . By contrast, in region IIb where $Q^2 < -\pi^2/H^2$, both kernels diverge with infinite real and imaginary parts [75]. This

$$\chi_{ij}(\omega) = \hbar c \int \frac{d^2 q}{(2\pi)^2} q_i q_j \left\{ [A_+(q, \omega) - A_+(q, 0)] |h_1(\mathbf{q})|^2 + \frac{1}{2} A_-(q, 0) (h_1(\mathbf{q})h_2(-\mathbf{q}) + h_1(-\mathbf{q})h_2(\mathbf{q})) \right\}, \quad (28)$$

and there is a residual force

$$f_i^0(\omega) = -\frac{\hbar c}{2} 2\pi \delta(\omega) \int \frac{d^2 q}{(2\pi)^2} i q_i A_-(q, 0) (h_1(\mathbf{q})h_2(-\mathbf{q}) - h_1(-\mathbf{q})h_2(\mathbf{q})). \quad (29)$$

expression for the effective action (after rotating back to real time), defined by $S_{\text{eff}} \equiv -i\hbar \ln \mathcal{Z}$, and eliminating h independent terms, is

H -dependent divergence extends all the way to the negative Q^2 axis, where it is switched off by a $1/H^5$ prefactor.

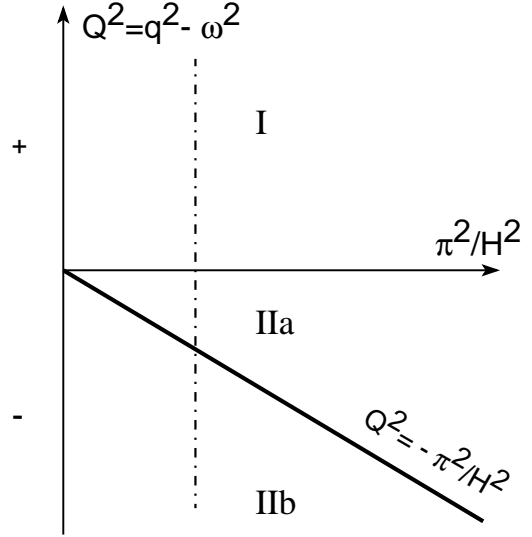


FIG. 2. Different regions of the (\mathbf{q}, ω) plane.

As a concrete example, let us examine the lateral vibration of plates with fixed roughness, such as two corrugated mirrors. The motion of the plates enters through the time dependencies $h_1(\mathbf{x}, t) = h_1(\mathbf{x} - \mathbf{r}(t))$ and $h_2(\mathbf{x}, t) = h_2(\mathbf{x})$; i.e. the first plate undergoes lateral motion described by $\mathbf{r}(t)$, while the second plate is stationary. The lateral force exerted on the first plate is obtained from $f_i(t) = \delta S_{\text{eff}} / \delta r_i(t)$. Within linear response, it is given by

$$f_i(\omega) = \chi_{ij}(\omega) r_j(\omega) + f_i^0(\omega), \quad (27)$$

where the “mechanical response tensor” is

VI. CORRUGATED MIRRORS

Let us now consider a corrugated plate with a deformation $h_1(\mathbf{x}) = d \cos(\mathbf{k} \cdot \mathbf{x})$. From the frequency-wavevector dependence of the mechanical response function in Eq.(28), we extract a plethora of interesting results, some of which we discuss next.

A. Mass corrections

For a single plate ($H \rightarrow \infty$), we can easily calculate the response tensor using the explicit formulas in Eq.(26). In the limit of $\omega \ll ck$, expanding the result in powers of ω gives $\chi_{ij} = \delta m_{ij} \omega^2 + O(\omega^4)$, where $\delta m_{ij} = A \hbar d^2 k^3 k_i k_j / (288 \pi^2 c)$, can be regarded as corrections to the mass of the plate. (Cut-off dependent mass corrections also appear, as in Ref. [60].) Note that these mass corrections are *anisotropic* with

$$\begin{aligned} \delta m_{\parallel} &= \frac{1}{288 \pi^2} \frac{\hbar}{c} A d^2 k^5, \\ \delta m_{\perp} &= 0. \end{aligned} \quad (30)$$

Parallel and perpendicular components are defined with respect to \mathbf{k} , and A denotes the area of the plates. The mass correction is inherently very small: For a macroscopic sample with $d \approx \lambda = 2\pi/k \approx 1\text{mm}$, density $\approx 15\text{gr/cm}^3$, and thickness $t \approx 1\text{mm}$, we find $\delta m/m \sim 10^{-34}$. Even for deformations of a microscopic sample of atomic dimensions (close to the limits of the applicability of our continuum representations of the boundaries), $\delta m/m$ can only be reduced to around 10^{-10} .

With the second plate at a separation H , the mass renormalization becomes a function of both k and H , with a crossover from the single plate behavior for $kH \sim 1$. In the limit of $kH \ll 1$, we obtain $\delta m_{\parallel} = \hbar A B k^2 d^2 / 48 c H^3$ and $\delta m_{\perp} = 0$, with $B = -0.453$. Compared to the single plate, there is an enhancement by a factor of $(kH)^{-3}$ in δm_{\parallel} . While the actual changes in mass are immeasurably small, the hope is that its *anisotropy* may be more accessible, say by comparing oscillation frequencies of a plate in two orthogonal directions.

B. Dissipation:

For $\omega \gg ck$ the response function is imaginary, and we define a frequency dependent effective shear viscosity by $\chi_{ij}(\omega) = -i\omega \eta_{ij}(\omega)$. This viscosity is also anisotropic, with

$$\begin{aligned} \eta_{\parallel}(\omega) &= \frac{1}{720 \pi^2} \frac{\hbar}{c^4} A d^2 k^2 \omega^4, \\ \eta_{\perp}(\omega) &= 0. \end{aligned} \quad (31)$$

Note that the dissipation is proportional to the fifth time derivative of displacement, and there is no dissipation for a uniformly accelerating plate. However, a freely oscillating plate will undergo a damping of its motion. The characteristic decay time for a plate of mass M is $\tau \approx 2M/\eta$. For the macroscopic plate of the previous paragraph, vibrating at a frequency of $\omega \approx 2ck$ (in the 10^{12}Hz range), the decay time is enormous, $\tau \sim 10^{18}\text{s}$. However, since the decay time scales as the fifth power of the dimension, it can be reduced to 10^{-12}s , for plates of order of 10 atoms. However, the required frequencies in this case (in the 10^{18}Hz range) are very large. Also note that for the linearized forms to remain valid in this high frequency regime, we must require very small amplitudes, so that the typical velocities involved $v \sim r_0 \omega$, are smaller than the speed of light. The effective dissipation in region IIa of Fig. 2 is simply the sum of those due to individual plates, and contains no H dependence.

C. Resonant Emission:

The cavity formed between the two plates supports a continuous spectrum of normal modes for frequencies $\omega^2 > c^2(k^2 + \pi^2/H^2)$. We find that both real and imaginary parts of $A_{\pm}(k, \omega)$, diverge in this regime, which we interpret as resonant dissipation due to excitation of photons in the cavity. Resonant dissipation has profound consequences for motion of plates. It implies that due to quantum fluctuations of vacuum, *components of motion with frequencies in the range of divergences cannot be generated by any finite external force!* The imaginary parts of the kernels are proportional to the total number of excited photons [58]. Exciting these degrees of motion must be accompanied by the generation of an infinite number of photons, requiring an infinite amount of energy, and thus impossible. However, as pointed out in Ref. [58], the divergence is rounded off by assuming finite reflectivity and transmissivity for the mirrors. Hence, in practice, the restriction is softened and controlled by the degree of ideality of the mirrors in the frequency region of interest.

Related effects have been reported in the literature for 1+1 dimensions [56–59], but occurring at a *discrete* set of frequencies $\omega_n = n\pi c/H$, with integer $n \geq 2$. These resonances occur when the frequency of the external perturbation matches the natural normal modes of the cavity, thus exciting quanta of such modes. In one space dimension, such modes are characterized by a discrete set of wavevectors that are integer multiples of π/H . The restriction to $n \geq 2$ is a consequence of quantum electrodynamics being a ‘free’ theory (quadratic action): only two-photon states can be excited subject to conservation of energy. Thus the sum of the frequencies of the two photons should add up to the external frequency [58]. In higher dimensions, the appropriate parameter is the combination $\omega^2/c^2 - q^2$. From the perspective of the ex-

cited photons, conservation of momentum requires that their two momenta add up to q , while energy conservation restricts the sum of their frequencies to ω . The in-plane momentum q , introduces a continuous degree of freedom: the resonance condition can now be satisfied for a continuous spectrum, in analogy with optical resonators. In Ref. [58], the lowest resonance frequency is found to be $2\pi c/H$ which seems to contradict our prediction. However, the absence of $\omega_1 = \pi c/H$ in 1+1 D is due to a vanishing prefactor [58], which is also present in our calculations. However, in exploring the continuous frequency spectrum in higher dimensions, this single point is easily bypassed, and there is a divergence for all frequencies satisfying $\omega^2/c^2 > q^2 + \pi^2/H^2$, where the inequality holds in its strict sense.

D. Radiation spectra

Where does the energy go when the plates experience viscous dissipation? When the viscosity is a result of losses in the dielectric boundaries [66–70], the energy is used up in heating the plates. Since we have examined perfect mirrors, the dissipated energy can only be accounted for by the emission of photons into the cavity. The path integral methods can be further exploited to calculate the spectrum of the emitted radiation [76]. The basic idea is to relate the transition amplitude from an empty vacuum (at $t \rightarrow -\infty$) to a state with two photons (at $t \rightarrow +\infty$), to two point correlation functions of the field, which is then calculated perturbatively in the deformations. From the transition amplitude (after integrating over the states of one photon) we obtain the probability that an emitted photon is observed at a frequency Ω , and a particular orientation.

Specifically, calculations of the angular distribution and spectrum of radiation were performed [76] for a single perfectly reflecting plate, undulating harmonically with a frequency ω_0 , and a wavevector \mathbf{k}_0 . Depending on the ratio ω_0/k_0 , we find that radiation at a frequency Ω is restricted to a particular window in solid angle. The total spectrum of radiation is found by integrating the angular distribution over the unit sphere, and is a sym-

metric function with respect to $\omega_0/2$, where it is peaked. The peak sharpens as the parameter $\omega_0/k_0 \rightarrow 0$, and saturates for $k_0 = 0$.

The connection between the dissipative dynamic Casimir force, and radiation of photons, is made explicit by calculating the total number of photons radiated per unit time and per unit area of the plate. The result is identical to the energy dissipation rate calculated in Ref. [73]. No radiation is observed at frequencies higher than ω_0 , due to conservation of energy, and also for $\omega_0/k_0 < 1$, in agreement with section B above, where no dissipative forces are found in this regime.

ACKNOWLEDGMENTS

We have benefitted from collaborations on these problems with M. Goulian, H. Li, M. Lyra, and F. Miri. MK is supported by the NSF grant DMR-93-03667. RG acknowledges many helpful discussions with J. Indekeu, and T. Liverpool, and support from the Institute for Advanced Studies in Basic Sciences, Gava Zang, Zanjan, Iran.

APPENDIX A: PATH-INTEGRAL FORMULATION AND DEFORMED SURFACES

In this Appendix, we sketch the path integral formulation developed in Ref. [15] for surfaces with roughness. Consider n manifolds embedded in a d -dimensional correlated fluid, with an energy cost appropriately generalized from Eq.(3). The manifolds are described by the functions $R_\alpha(x_\alpha)$, where x_α is a D_α -dimensional internal coordinate ($D_\alpha = 1$ for a polymer, and $D_\alpha = 2$ for a membrane), while R_α indicates a position in the d -dimensional fluid. The fluctuation-induced interactions between the manifolds are obtained by integrating over all configurations of the field ϕ , subject to the constraints of its vanishing on the external manifolds. The boundary conditions ($\phi(R_\alpha(x_\alpha)) = 0$, for $\alpha = 1, 2, \dots, n$) are imposed by inserting delta functions. Using the integral representation of the delta function, we can write

$$\exp\left(-\frac{\mathcal{H}_{eff}}{k_B T}\right) = \frac{1}{\mathcal{Z}_0} \int \mathcal{D}\phi(r) \prod_{\alpha=1}^n \mathcal{D}\psi_\alpha(x_\alpha) \exp\left(-\mathcal{H}_0[\phi] + i \int dx_\alpha \psi_\alpha(x_\alpha) \phi(R_\alpha(x_\alpha))\right), \quad (1)$$

where $\psi_\alpha(x_\alpha)$ are the auxiliary fields defined on the n manifolds, acting as sources coupled to ϕ . For the quadratic Hamiltonian of Eq.(3), it is easy to integrate over the field ϕ , and obtain the long-range interactions between the sources as

$$\exp\left(-\frac{\mathcal{H}_{eff}}{k_B T}\right) = \int \prod_{\alpha=1}^n \mathcal{D}\psi_\alpha(x_\alpha) \exp(-\mathcal{H}_1[\psi_\alpha(x_\alpha)]) . \quad (2)$$

The action $\mathcal{H}_1[\psi_\alpha(x_\alpha)]$ is a quadratic form for the n component field $\Psi \equiv (\psi_1, \psi_2, \dots, \psi_n)$, given by

$$\mathcal{H}_1[\Psi] \equiv \Psi M \Psi^T = \sum_{\alpha=1}^n \sum_{\beta=1}^n \int dx_\alpha dy_\beta \psi_\alpha(x_\alpha) G^d(R_\alpha(x_\alpha) - R_\beta(y_\beta)) \psi_\beta(y_\beta), \quad (3)$$

where $G^d(r) \equiv \langle \phi(r)\phi(0) \rangle_0$ is the two-point correlation function of the field ϕ in free space. Finally, the effective interaction between the manifolds is obtained by performing the Gaussian integrations over the field Ψ as

$$\mathcal{H}_{eff}[R_\alpha(x_\alpha)] = \frac{k_B T}{2} \ln \det(M[R_\alpha(x_\alpha)]) . \quad (4)$$

The matrix M (which can be read off from Eq.(3)) is a functional of $R_\alpha(x_\alpha)$ and its determinant is in general difficult to evaluate for arbitrary configurations. It is possible, however, to perturbatively calculate the corrections due to small deformations around simple base configurations. Consider two surfaces in $d = 3$, with average separation H . One plate has small deformations described by $h(\mathbf{x})$, i.e. $R_1(\mathbf{x}) = (x_1, x_2, 0)$, while

$$\mathcal{H}_{corr} = -k_B T \times \frac{3\zeta(3)}{16\pi H^4} \int d^2 \mathbf{x} h^2(\mathbf{x}) + \frac{k_B T}{4} \int d^2 \mathbf{x} d^2 \mathbf{y} [h(\mathbf{x}) - h(\mathbf{y})]^2 \times \left\{ \frac{1}{8\pi^2 |\mathbf{x} - \mathbf{y}|^6} + \frac{1}{2\pi |\mathbf{x} - \mathbf{y}|^3 H^3} K_1 \left(\frac{|\mathbf{x} - \mathbf{y}|}{H} \right) + \frac{1}{H^6} \left[K_1 \left(\frac{|\mathbf{x} - \mathbf{y}|}{H} \right) \right]^2 + \frac{1}{H^6} \left[K_2 \left(\frac{|\mathbf{x} - \mathbf{y}|}{H} \right) \right]^2 \right\} , \quad (6)$$

with two kernel functions defined by

$$K_1(t) \equiv \int_0^\infty \frac{du}{2\pi} u^2 (e^{2u} - 1)^{-1} J_0(tu), \quad (7)$$

$$K_2(t) \equiv \int_0^\infty \frac{du}{2\pi} u^2 e^u (e^{2u} - 1)^{-1} J_0(tu). \quad (8)$$

The first term in Eq.(6) represents an instability to deformations that is related to the attraction between the plates. Remarkably, this term can be obtained intuitively by replacing $1/H^2$ with $1/(H + h(\mathbf{x}))^2$ in Eq.(5) and averaging over the position \mathbf{x} . The second term represents long-range interactions between the deformations, induced by the fluctuations of the field. The first term in the curly brackets is the conformation energy of the deformed surface in the absence of the second plane, and is independent of H . The remaining terms represent correlations due to the presence of second plane. Both $K_1(t)$ and $K_2(t)$ approach a constant as $t \rightarrow 0$. As $t \rightarrow \infty$, $K_1(t) \sim 1/t^3$, while $K_2(t) \sim \exp(-bt)$, with $b \approx 3.3$. The large t behaviors of $K_1(t)$ and $K_2(t)$ determine the long-range interactions between height fluctuations.

APPENDIX II: PATH INTEGRAL FORMULATION OF CHARGED FLUIDS

Here, we introduce a systematic path integral formulation to study fluctuation-induced interactions in a charged fluid. Consider n charged manifolds embedded in a d -dimensional aqueous solution of neutralizing counterions, interacting through Coulomb potentials. The manifolds have charge densities $-\sigma_\alpha$ (all assumed to be

$$e^{-H_C/k_B T} = \int \mathcal{D}\phi(X) \exp \left\{ -\frac{\epsilon k_B T}{2S_d e^2} \int d^d X (\nabla\phi)^2 + i \int d^d X \rho(X) \phi(X) \right\} , \quad (4)$$

we can rewrite the partition function as

$R_2(\mathbf{x}) = (x_1, x_2, H + h(\mathbf{x}))$. The effective Hamiltonian can now be written as $\mathcal{H}_{eff} = \mathcal{H}_{flat} + \mathcal{H}_{corr}$, where \mathcal{H}_{flat} is the Casimir interaction for two flat plates, and \mathcal{H}_{corr} is the additional cost of deformations. For flat plates of area A , the interaction energy is

$$\frac{\mathcal{H}_{flat}}{A} = k_B T \int \frac{d^2 \mathbf{p}}{(2\pi)^2} \ln \left(\frac{1}{2\alpha p} \right) - \frac{\zeta(3)}{16\pi} \frac{k_B T}{H^2} . \quad (5)$$

The first term in Eq.(5) is a contribution to the surface tension which depends on a lattice cutoff. The second term is the usual Casimir interaction, decaying as $1/H^2$, and with a universal amplitude $-\zeta(3)/16\pi \approx -0.02391$.

The energy cost of deformations is given by

negatively charged for simplicity), and are described by the functions $R_\alpha(x_\alpha)$, where x_α is a D_α -dimensional internal coordinate, while R_α indicates a position in the d -dimensional solution. There are N_c positively charged counterions of valence z , each described by a position vector R_i , in the d -dimensional solution. The Coulomb Hamiltonian can be written as

$$H_C = \frac{1}{2} \int d^d X d^d X' \rho(X) \frac{e^2}{\epsilon |X - X'|^{d-2}} \rho(X'), \quad (1)$$

where

$$\rho(X) = - \sum_{\alpha=1}^n \int dx_\alpha \sigma_\alpha \delta^d(X - R_\alpha(x_\alpha)) + \sum_{i=1}^{N_c} z \delta^d(X - R_i), \quad (2)$$

is the number density of the charges. Charge neutrality requires $-\sum_{\alpha=1}^n \sigma_\alpha A_\alpha + z N_c = 0$, where A_α is the D_α -dimensional area of the α th manifold.

A restricted partition function of the Coulomb system, depending upon the shapes and locations of the macromolecules, is now given by

$$\mathcal{Z}_{N_c}[R_\alpha(x_\alpha)] = \int \prod_{i=1}^{N_c} \frac{d^d R_i}{a^d} e^{-H_C/k_B T}, \quad (3)$$

in which a is a short-distance cut-off. Using the Hubbard-Stratanovich transformation of the Coulomb interaction,

$$\mathcal{Z}_{N_c}[R_\alpha(x_\alpha)] = \int \mathcal{D}\phi(X) \exp \left\{ -\frac{\epsilon k_B T}{2S_d e^2} \int d^d X (\nabla\phi)^2 - i \sum_{\alpha=1}^n \int dx_\alpha \sigma_\alpha \phi(R_\alpha(x_\alpha)) \right\} \left(\int \frac{d^d R}{a^d} e^{iz\phi(R)} \right)^{N_c}, \quad (5)$$

where S_d is the area of the d -dimensional unit sphere. We can introduce a fugacity y , and a rescaled partition function

$$\mathcal{Z}[R_\alpha(x_\alpha)] = \frac{y^{N_c}}{N_c!} \mathcal{Z}_{N_c}[R_\alpha(x_\alpha)], \quad (6)$$

that can be rewritten as

$$\begin{aligned} \mathcal{Z} &= \sum_{N=0}^{\infty} \delta_{N,N_c} \frac{y^N}{N!} \mathcal{Z}_N[R_\alpha(x_\alpha)] \\ &= \sum_{N=0}^{\infty} \int_0^{2\pi} \frac{d\theta}{2\pi} e^{i\theta(N_c-N)} \int \mathcal{D}\phi(X) \exp \left\{ -\frac{\epsilon k_B T}{2S_d e^2} \int d^d X (\nabla\phi)^2 - i \sum_{\alpha=1}^n \int dx_\alpha \sigma_\alpha \phi(R_\alpha(x_\alpha)) \right\} \frac{1}{N!} \left(y \int \frac{d^d R}{a^d} e^{iz\phi(R)} \right)^N. \end{aligned} \quad (7)$$

A shift in the field ϕ by $-\theta$, and use of the neutrality condition renders the θ -integration trivial. We can then sum up the exponential series, and obtain

$$\mathcal{Z}[R_\alpha(x_\alpha)] = \int \mathcal{D}\phi(X) e^{-\mathcal{H}[\phi]}, \quad (8)$$

in which

$$\mathcal{H}[\phi] = \frac{\epsilon k_B T}{2S_d e^2} \int d^d X (\nabla\phi)^2 + i \sum_{\alpha=1}^n \int dx_\alpha \sigma_\alpha \phi(R_\alpha(x_\alpha)) - \frac{y}{a^d} \int d^d X e^{iz\phi(X)}. \quad (9)$$

Note that the fugacity y can be eliminated using the identity

$$N_c = y \frac{\partial \ln \mathcal{Z}}{\partial y}, \quad (10)$$

which follows from Eq.(6).

We next evaluate the path integral using a saddle point approximation. The extremum of Eq.(8), obtained from $\delta\mathcal{H}/\delta\phi = 0$, is the solution of the Poisson-Boltzmann (PB) equation

$$-\nabla^2(z\psi(X)) - \kappa^2 e^{-z\psi(X)} = - \sum_{\alpha=1}^n \int dx_\alpha \frac{S_d e^{2z\sigma_\alpha}}{\epsilon k_B T} \delta^d(X - R_\alpha(x_\alpha)), \quad (11)$$

for the (real) field $\psi(X) = -i\bar{\phi}(X)$, in which $\kappa^2 = S_d e^{2z} y z^2 / \epsilon k_B T a^d$ defines the inverse square of the Debye screening length. To study the fluctuations on top of this saddle point, we can set $\phi = \bar{\phi} + \delta\phi$, and expand the Hamiltonian up to quadratic order, to get

$$\mathcal{H}[\phi] = \mathcal{H}[\bar{\phi}] + \frac{\epsilon k_B T}{2S_d e^2} \int d^d X \left[(\nabla\delta\phi)^2 + \kappa^2 e^{-z\psi(X)} \delta\phi^2 \right]. \quad (12)$$

The free energy of the system of charged manifolds in the presence of fluctuating counterions now reads

$$F = F_{PB} + \frac{k_B T}{2} \ln \det [-\nabla^2 + m^2(X)], \quad (13)$$

where $F_{PB} = \mathcal{H}[i\psi(X)]$ is the Poisson-Boltzmann free energy, and $m^2(X) = \kappa^2 e^{-z\psi(X)}$ is a ‘‘mass (or charge compressibility) profile’’. The PB free energy is known to be generically repulsive [35,26]. The fluctuation-induced correction, however, is attractive. For highly charged manifolds, it is indeed reminiscent of the Casimir interac-

tions, but with the boundary constraints smoothed out. To see this, one should note that the mass profile is indeed identical to the density profile of the counterions. Highly charged manifolds accumulate counterions in their vicinity, and consequently the fluctuations of the ‘‘potential’’ field ϕ are suppressed in a region close to the manifolds, but are unconstrained in other regions in the solution; hence leading to a Casimir-type fluctuation-induced attraction.

- [1] H.B.G. Casimir, Proc. K. Ned. Akad. Wet. **51**, 793 (1948).
- [2] I.E. Dzyaloshinskii, E.M. Lifshitz, and L.P. Pitaevskii, Advan. Phys. **10**, 165 (1961).
- [3] V.M. Mostepanenko and N.N. Trunov, *The Casimir Effect and Its Applications* (Clarendon Press, Oxford, 1997).
- [4] M. Krech, *The Casimir Effect in Critical Systems* (World Scientific, Singapore, 1994).
- [5] S. Weinberg, Rev. Mod. Phys. **61**, 1 (1989).
- [6] I.I. Abricossova and B.V. Deryaguin, Dokl. Akad. Nauk. SSSR **90**, 1055 (1953).
- [7] M.J. Sparnaay, Physica **24**, 751 (1958).
- [8] See, e.g. J.N. Israelachvili and P.M. McGuigan, Science **241**, 6546 (1990).
- [9] S.K. Lamoreaux, Phys. Rev. Lett. **78**, 5 (1997).
- [10] M.E. Fisher and P.-G. de Gennes, C. R. Acad. Sci. Ser. B **287**, 207 (1978); V. Privman and M.E. Fisher, Phys. Rev. B **30**, 322 (1984).
- [11] H.W.J. Blöte, J.L. Cardy, and M.P. Nightingale, Phys. Rev. Lett. **56**, 742 (1986).
- [12] M.P. Nightingale and J.O. Indekeu, Phys. Rev. Lett. **54**, 1824 (1985).
- [13] M. Krech and S. Dietrich, Phys. Rev. Lett. **66**, 345 (1991).
- [14] For a study of phonon fluctuation-induced interactions, see N.K. Mahale and M.W. Cole, Surf. Sci. **172**, 311 (1986).
- [15] H. Li and M. Kardar, Phys. Rev. Lett. **67**, 3275 (1991); Phys. Rev. A **46**, 6490 (1992).
- [16] J. Schwinger, L.L. DeRaad, and K.A. Milton, Ann. Phys. (N.Y.) **115**, 1 (1978).
- [17] For a review see, e.g., S. Dietrich, in *Phase Transitions and Critical Phenomena*, edited by C. Domb and J.L. Lebowitz (Academic, New York, 1988), vol.12.
- [18] For liquid Helium films with thickness of more than 100\AA , the van der Waals interaction is retarded, and falls off as $1/H^3$, to leading order. In this case, the expression for the film thickness is more complicated, and will not be elaborated on here.
- [19] J. Indekeu, J. Chem. Soc. Faraday Trans. II **82**, 1835 (1986).
- [20] K.K. Mon and M.P. Nightingale Phys. Rev. B **35**, 3560 (1987).
- [21] M. Chan and R. Garcia, private communication (1998).
- [22] P.-G. de Gennes, *The physics of Liquid Crystals* (Oxford Univ. Press, Oxford, 1974).
- [23] L.V. Mikheev, Sov. Phys. JETP **69**, 358 (1989).
- [24] A. Ajdari, L. Peliti and J. Prost, Phys. Rev. Lett. **66**, 1481 (1991).
- [25] M.L. Lyra, M. Kardar, and N.F. Svatier, Phys. Rev. E. **47**, 3456 (1993).
- [26] F. Oosawa, Biopolymers **6**, 134 (1968); *Polyelectrolytes* (Marcel Dekker, New York, 1971).
- [27] S. Marcelja, Biophys. J. **61**, 1117 (1992), and references therein.
- [28] P. Attard, J. Mitchell, and B.W. Ninham, J. Chem. Phys. **88**, 4987 (1988).
- [29] See for example, Ref. [28] and references therein.
- [30] P. Attard, R. Kjellander, and D.J. Mitchell, Chem. Phys. Lett. **139**, 219 (1987); P. Attard, R. Kjellander, D.J. Mitchell, and B. Jönsson, J. Chem. Phys. **89**, 1664 (1988).
- [31] The calculation of the determinant using the true compressibility profile for the Casimir geometry has indeed been carried out in Ref. [28], with the result
- $$F_{FI} = -k_B T \times \frac{A}{H^2} \times \left[\frac{\zeta(3)}{16\pi} + \frac{\pi}{4} \left(\frac{\pi}{4} + \frac{1}{2} \right) + \frac{\pi}{4} \ln(2z\ell_B\sigma H) + O(\xi/H) \right].$$
- It is interesting to note that the correct result is considerably stronger than that of the simple ‘‘Gouy-Chapman’’ model (Eq.(12)).
- [32] H.B.G. Casimir and D. Polder, Phys. Rev. **73**, 360 (1948).
- [33] F. London, Z. Phys. Chem. B **11**, 222 (1930).
- [34] D. Kleppner, Physics Today, October 1990, page 9.
- [35] J. Israelachvili, *Intermolecular and Surface Forces* (Academic Press, San Diego 1992).
- [36] O.G. Mouritsen and M. Bloom, Annu. Rev. Biophys. Biomol. Struct. **22**, 145 (1993).
- [37] M. Goulian, R. Bruinsma, and P. Pincus, Europhys. Lett. **22**, 145 (1993); Erratum in Europhys. Lett. **23**, 155 (1993).
- [38] N. Dan, P. Pincus, and S.A. Safran, Langmuir **9**, 2768 (1993).
- [39] P.B. Canham, J. Theor. Biol. **26**, 61 (1970); W. Helfrich, Z. Naturforsch. **28c**, 693 (1973).
- [40] P.G. de Gennes and C. Taupin, J. Phys. Chem. **86**, 2294 (1982).
- [41] F. Brochard and J.F. Lennon, J. de Phys. **36**, 1035 (1975).
- [42] F. David and S. Leibler, J. de Phys. II **1**, 959 (1991).
- [43] R. Golestanian, M. Goulian, and M. Kardar, Europhys. Lett. **33**, 241 (1996); Phys. Rev. E **54**, 6725 (1996).
- [44] In this formula, the result in Ref. [37] has been corrected by a factor of 1/2 [43].
- [45] E. D’Hoker, P. Sikivie, and Y. Kanev, Phys. Lett. B **347**, 56 (1995).
- [46] R. Golestanian, Europhys. Lett. **36**, 557 (1996).
- [47] R. Balian and B. Duplantier, Annals of Phys. **112**, 165 (1978).
- [48] M. Yu. Novikov, A.S. Sorin, and V. Ya. Chernyak, Teor. Mat. Fiz. **82**, 178 (1990); *ibid.* **82**, 360 (1990); *ibid.* **91**, 474 (1992); *ibid.* **92**, 113 (1992).
- [49] M. Bordag, G.L. Klimchitskaya, and V.M. Mostepanenko, Int. J. Mod. Phys. A **10**, 2661 (1995).
- [50] L.H. Ford and A. Vilenkin, Phys. Rev. D **25**, 2569 (1982).
- [51] M. Kardar, in *Proceedings of the 4th International Conference on Surface X-Ray and Neutron Scattering*, eds. G.p. Felcher and H. You, Physica B **221**, 60 (1996).
- [52] G.T. Moore, J. Math. Phys. **11**, 2679 (1970).
- [53] S.A. Fulling, and P.C.W. Davies, Proc. R. Soc. A **348**, 393 (1976).
- [54] M.-T. Jaekel, and S. Reynaud, Phys. Lett. A **167**, 227 (1992).
- [55] P.A. Maia Neto, and S. Reynaud, Phys. Rev. A **47**, 1639 (1993).
- [56] G. Calucci, J. Phys. A: Math. Gen. **25**, 3873 (1992); C.K.

- Law, Phys. Rev. A **49**, 433 (1994); V.V. Dodonov, Phys. Lett. A **207**, 126 (1995).
- [57] O. Meplan and C. Gignoux, Phys. Rev. Lett. **76**, 408 (1996).
- [58] A. Lambrecht, M.-T. Jaekel, and S. Reynaud, Phys. Rev. Lett. **77**, 615 (1996).
- [59] P. Davis, Nature **382**, 761 (1996).
- [60] G. Barton and C. Eberlein, Ann. Phys. (N.Y.) **227**, 222 (1993).
- [61] J. Schwinger, Proc. Natl. Acad. Sci. USA **89**, 4091 (1992); **90**, 958 (1993); **91**, 6473 (1994).
- [62] C. Eberlein, Phys. Rev. Lett. **76**, 3842 (1996); Phys. Rev. A **53**, 2772 (1996).
- [63] P. Knight, Nature **381**, 736 (1996).
- [64] B. Gompf *et al.*, Phys. Rev. Lett. **79**, 1405 (1997); R.A. Hiller, S.J. Putterman, and K.R. Weninger, Phys. Rev. Lett. **80**, 1091 (1998).
- [65] V.V. Dodonov, A.B. Klimov, and V.I. Man'ko, Phys. Lett. A **142**, 511 (1989).
- [66] L.S. Levitov, Europhys. Lett. **8**, 499 (1989).
- [67] V.E. Mkrtchian, Phys. Lett. A **207**, 299 (1995).
- [68] G. Barton, Ann. Phys. (N.Y.) **245**, 361 (1996).
- [69] J.B. Pendry, J. Phys. Condens. Matter **9**, 10301 (1997).
- [70] C. Eberlein, Phys. World, **11**, 27 (1998).
- [71] A. Dayo, W. Alnasrallah, and J. Krim, Phys. Rev. Lett. **80**, 1690 (1998).
- [72] G.E. Volovik, Pisma ZhETF **63**, 457 (1996); JETP Lett. **63**, 483 (1996).
- [73] R. Golestanian and M. Kardar, Phys. Rev. Lett. **78**, 3421 (1997); submitted to Phys. Rev. A (1998), cond-mat 9802017.
- [74] For two plates separated by H , the perturbation series is in the small parameters h_1/H and h_2/H . For a single plate ($H \rightarrow \infty$), the requirement is that the time and space derivatives of the height functions should be small.
- [75] The divergence of kernels in IIb comes from integrations over space-time. Given a cut-off L in plate size, and an associated cutoff L/c in time, the kernels diverge as $\exp[(K-2)L/H]/[K(L/H)^3]$, with $K = 2QH/\pi$. Some care is necessary in the order of limits for $(L, H) \rightarrow \infty$.
- [76] F. Miri, R. Golestanian, and M. Kardar, in preparation.